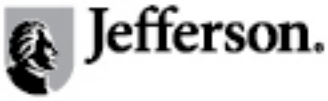

November 2005

Continuous ASL perfusion fMRI investigation of higher cognition: Quantification of tonic CBF changes during sustained attention and working memory tasks

Junghoon Kim
Albert Einstein Healthcare Network and University of Pennsylvania

John Whyte
Thomas Jefferson University and Albert Einstein Healthcare Network, whytej@einstein.edu

Jiongjiong Wang
University of Pennsylvania

Hengyi Rao
University of Pennsylvania

Kathy Z. Tang
University of Pennsylvania

See next page for additional authors

Authors
Junghoon Kim, John Whyte, Jiongjiong Wang, Hengyi Rao, Kathy Z. Tang, and John A. Detre

Continuous ASL perfusion fMRI investigation of higher cognition: Quantification of tonic CBF changes during sustained attention and working memory tasks

Junghoon Kim,[a,b] * John Whyte,[a,c] Jiongjiong Wang,[b,d,e] Hengyi Rao,[b] Kathy Z. Tang,[b] and John A. Detre[b,d,e]

[a] Moss Rehabilitation Research Institute, Albert Einstein Healthcare Network, 1200 W. Tabor Road, Philadelphia, PA 19141, USA

[b] Center for Functional Neuroimaging, University of Pennsylvania, Philadelphia, PA 19104, USA

[c] Department of Rehabilitation Medicine, Thomas Jefferson University, Philadelphia, PA 19107, USA

[d] Department of Neurology, University of Pennsylvania, Philadelphia, PA 19104

[e] Department of Radiology, University of Pennsylvania, Philadelphia, PA 19104, USA

* Corresponding author. Moss Rehabilitation Research Institute, 1200 W. Tabor Road, Philadelphia, PA 19141, USA. Fax: +1 215 456 5926.
E-mail address: kimj@einstein.edu (J.Kim).

Abstract

Arterial spin labeling (ASL) perfusion fMRI is an emerging method in clinical neuroimaging. Its non-invasiveness, absence of low frequency noise, and ability to quantify the absolute level of cerebral blood flow (CBF) make the method ideal for longitudinal designs or low frequency paradigms. Despite the usefulness in the study of cognitive dysfunctions in clinical populations, perfusion activation studies to date have been conducted for simple sensorimotor paradigms or with single-slice acquisition, mainly due to technical challenges. Using our recently developed amplitude-modulated continuous ASL (CASL) perfusion fMRI protocol, we assessed the feasibility of a higher level cognitive activation study in twelve healthy subjects. Taking advantage of the ASL noise properties, we were able to study tonic CBF changes during uninterrupted 6-min continuous performance of working memory and sustained attention tasks. For the visual sustained attention task, regional CBF increases (6–12 ml/100 g/min) were detected in the right middle frontal gyrus, the bilateral occipital gyri, and the anterior cingulate/medial frontal gyri. During the 2-back working memory task, significantly increased activations (7–11 ml/100 g/min) were found in the left inferior frontal/precentral gyri, the left inferior parietal lobule, the anterior cingulate/medial frontal gyri, and the left occipital gyrus. Locations of activated and deactivated areas largely concur with previous PET and BOLD fMRI studies utilizing similar paradigms. These results demonstrate that CASL perfusion fMRI can be successfully utilized for the investigation of the tonic CBF changes associated with high level cognitive operations. Increased applications of the method to the investigation of cognitively impaired populations are expected to follow.

Keywords: Arterial spin labeling; CASL; Cerebral blood flow; 2-back task; Clinical neuroimaging

Introduction

During the past decade, functional magnetic resonance imaging (fMRI) has become a standard tool for visualizing resting and task-related brain activations. In comparison to positron emission tomography (PET) or single photon emission computed tomography (SPECT), fMRI has higher spatial and temporal resolution, does not involve exposure to ionizing radiation, and is widely available at medical centers. These merits have expanded the applications of fMRI to many clinical areas including presurgical mapping, psychopharmacology, and pediatric neuroimaging (Detre and Floyd, 2001; Hennig et al., 2003; Honey and Bullmore, 2004; Matthews and Jezzard, 2004; Wilke et al., 2003). Blood-oxygenation-level-dependent (BOLD) fMRI has been the method of choice in most occasions, due to its high sensitivity to task-related effects and relative ease of implementation. However, BOLD contrast is known to be a

complex interaction of multiple physiological parameters including blood flow, blood volume, and hemoglobin oxygenation (Kwong et al., 1992; Mandeville et al., 1999; Ogawa et al., 1993). As a result, it confounds changes from neuronal activation with vascular effects, making the interpretation of data difficult when circulatory changes are expected due to cerebrovascular disease or direct vascular effects of pharmacological intervention. Lack of an absolute measure of cerebral blood flow also limits the application of BOLD fMRI in situations where multiple scanning sessions need to be compared since condition differences can arise due to either (or both) an increase in activation or a decrease in deactivation (e.g., Poldrack, 2000). In addition, the presence of low frequency noise in the BOLD signal (Friston et al., 2000; Zarahn et al., 1997) precludes using a long task block (e.g., >2 min), making it difficult to investigate slow processes such as learning, emotion, and sustained attention in healthy and clinical populations.

Arterial spin labeling (ASL) fMRI is an emerging methodology that uses magnetically labeled arterial blood water as an endogenous tracer to provide quantitative cerebral blood flow (CBF) measurements (Detre et al., 1992; Williams et al., 1992). This non-invasive method provides highly reliable measures of CBF, making it particularly suitable for longitudinal studies of treatment (e.g., drug or training) effects or functional recovery processes that require assessment of baseline function and repeated measurements across sessions (Detre and Alsop, 1999; Detre and Wang, 2002). ASL contrast, due to the pairwise subtraction of temporally adjacent images, is also free from the slow signal drifts present in BOLD fMRI contrast (Aguirre et al., 2002). As a result, it is well suited for investigating low frequency brain events such as changes related to practice, mood, and mental set (Wang et al., 2003a,b). In addition, recent evidence suggests that ASL fMRI may provide contrasts with smaller intersubject variability (Aguirre et al., 2002; Kemeny et al., 2005), reduced susceptibility artifacts in regions of high static inhomogeneity (Tjandra et al., 2005; Wang et al., 2004), and more specific functional localization than BOLD fMRI (Duong et al., 2001; Luh et al., 2000).

Due to the advantageous characteristics mentioned above, ASL perfusion fMRI has been increasingly adopted for clinical studies of cerebral perfusion during resting states (e.g., Ances et al., 2004; Johnson et al., 2005; Oguz et al., 2003; Rashid et al., 2004). However, few studies have attempted to validate this technique with cognitive activation paradigms. Previous activation studies have mainly used passive visual stimulation (Aguirre et al., 2002; Talagala and Noll, 1998) or simple psychomotor tasks such as finger tapping (Garraux et al., 2005; Mildner et al., 2003; Wang et al., 2003a,b). Only two studies to date have used cognitive paradigms such as the 2-back and verb generation tasks (Ye et al., 1998; Yee et al., 2000). However, these studies acquired only single slices, limiting their use to hypothesis testing regarding a priori regions-of-interest (ROIs). Thus, a whole-brain multi-slice study with conventional voxelwise group analyses is needed to validate ASL pefusion fMRI for the investigation of the widely distributed neural networks of high-level cognitive processes such as attention and working memory.

It is known from previous PET studies that there are significantly smaller CBF changes during cognitive activation tasks compared to those during simple sensory–motor tasks (Colebatch et al., 1991; Jonides et al., 1997; Paulesu et al., 1993; Ramsey et al., 1996). Considering the relatively low signal-to-noise ratio (SNR) of ASL fMRI (cf. Calamante et al., 1999), detecting these subtle changes could be a major challenge for studies of higher cognitive processes using this method. The combination of high magnetic field strength and continuous ASL (CASL) method offers an appealing approach to improve the SNR and image coverage of ASL fMRI (Wang et al., 2002). One way of implementing a high-field ASL fMRI is to use a separate small RF coil for labeling (Mildner et al., 2003; Zaharchuk et al., 1999). However, this dual-coil approach requires special hardware and relies heavily on the labeling geometry, which may vary from subject to subject. The added distance for arterial transit from the carotid tagging region and the relatively poor labeling of the vertebral arteries also limit the practical use of this approach. Recently, we demonstrated that whole-brain multi-slice CASL fMRI could be successfully implemented with a single transmit–receive coil at 3.0 T by reducing RF pulses and gradient strength appropriately (Wang et al.,

2005). Our goal in the present study was to demonstrate that higher cognitive processes could be studied utilizing the same imaging protocol, with appropriate sensitivity and localization power.

Two cognitive tasks were selected to assess CASL fMRI's sensitivity to CBF changes related to high-level cognitive processes. Both tasks are known to be 'frontal' tasks–that is, they involve prefrontal areas for successful performance–by previous PET and BOLD fMRI investigations. The first task was a visual sustained attention task (Whyte et al., 1995). Since sustained attention is also implicated in various clinical disorders including attention deficit hyperactivity disorder, traumatic brain injury, and Alzheimer's disease, it is important to understand the neural correlates of this cognitive function. Previous neuroimaging studies of sustained attention in the visual modality have consistently identified a right hemisphere dominant fronto-parietal network (Coull et al., 1996, 1998; Lawrence et al., 2003; Pardo et al., 1991). However, these studies used rather short data acquisition blocks (40–90 s) that might not be optimal for detecting aspects of sustained attention associated with prolonged task performance. Taking advantage of ASL fMRI's noise characteristics, the current study was able to employ a long (6 min) block of uninterrupted performance of visual target detection. It was hypothesized that we would find tonic changes of CBF in the previously identified areas of the visual sustained attention network, including the right middle frontal and right parietal cortices.

The second task was a working memory (2-back) task (Cohen et al., 1997; Jonides et al., 1997). It is known from previous neuroimaging studies that various versions of this task invoke activations in a large-scale network including prefrontal, premotor, supplementary motor, and parietal cortices (Cabeza and Nyberg, 2000; D'Esposito et al., 1998; Smith and Jonides, 1998, 1999). Since this task is one of the most frequently used high-level cognitive tasks in various clinical populations (e.g., Callicott et al., 2003; Kwon et al., 2001; Scheibel et al., 2003; Sweet et al., 2004; Valera et al., 2005), implementing it with a whole-brain multi-slice ASL approach would provide useful comparison CBF data for future clinical neuroimaging studies. It was predicted that we would replicate the results from prior normative studies using the 2-back task (for review, see Owen et al., 2005).

Materials and methods

Participants

Seventeen healthy volunteers participated in this study. Five subjects were excluded from subsequent data analysis due to large head movements during scanning (see Imaging data analysis for the criteria). The remaining subjects included 9 men and 3 women aged between 21 and 46 years (mean age = 34.4 years, SD = 9.5) with a mean education of 13.3 years (SD = 2.0). Eleven of them were right-handed (Edinburgh Handedness Inventory, Oldfield, 1971). Subjects had no previous history of neurological or major psychiatric disorder and had normal or corrected-to-normal visual acuity. After complete description of the study, subjects provided written informed consent to the University of Pennsylvania Institutional Review Board-approved protocol.

Cognitive tasks

Visual sustained attention task

A simple go/no-go visual reaction time task was used to examine the neural network involved in maintaining visual sustained attention (Whyte et al., 1995, 2004). Stimuli consisted of pairs of vertical lines presented for a brief period in the center of the screen. The central area of the screen was covered by a random pattern mask with a fixation cross except when a stimulus was presented. The mask subtended approximately 1º and 4º of horizontal and vertical visual angle, respectively. Subjects were taught that a

pair of identical lines constituted a target, whereas a pair of grossly unequal lines constituted a foil (one line was the same length as the target and the other was 50% shorter), and to press the button with their dominant hand as quickly and accurately as possible in response to targets only. They were also explicitly told that only 20% of the stimuli were targets. A total of 60 stimuli were presented during an uninterrupted 6-min task block with an average interstimulus interval of 6 s (range: 4 to 8 s).

Two-back task

A letter version of 2-back task (Awh et al., 1996; Cohen et al., 1997) was employed to examine the neural network involved in continuous performance of a working memory task. In this task, subjects were presented with a series of letters in the center of the screen. The letters subtended approximately 1.5º × 1..5º of visual angle. Subjects were required to press the button whenever each letter presented was identical to the one presented two letters previously in the sequence. A total of 180 letters were presented with an exposure duration of 1 s and an interstimulus interval (ISI) of 2 s. The target rate for this task was 12%.

Experimental design and procedure

Prior to the scanning sessions, subjects were trained on the two tasks outside of the scanner. For the visual sustained attention task, stimulus exposure durations were individualized to avoid ceiling or floor performance level. Average stimulus exposure duration was 62.2 ms (SD = 21.2). Details of the calibration procedure are available elsewhere (Whyte et al., 1995). The order of task blocks was always resting first, the sustained attention task second, and the 2-back task last. Each task block was approximately 6 min, and the intervals between task blocks were approximately 30 s. During the resting condition, which was used as the baseline control, subjects were instructed to close their eyes but stay awake. For both tasks, responses and reaction times (RTs) were recorded for further analysis.

Imaging data acquisition

The functional imaging was conducted on a Siemens 3.0 T Trio whole-body scanner (Siemens AG, Erlangen, Germany), using a standard transmit–receive head coil. An amplitude-modulated CASL technique was implemented for perfusion fMRI scans (Wang et al., 2005). Interleaved images with and without labeling were acquired using a gradient echo echo-planar imaging sequence with the following acquisition parameters: FOV = 22 cm, matrix = 64 × 64, TR = 4 s, TE = 17 ms, flip angle = 90º. Fourteen slices (6 mm thickness with 1.5 mm gap) were acquired from inferior to superior in a sequential order to cover the whole brain. A delay time of 1 s was inserted between the end of labeling pulses and image acquisition to reduce transit-related effects. Each subject performed three CASL scans each with 92 acquisitions (approximately 6 min). Before the functional scans, high resolution T1-weighted anatomic images were obtained using 3D MPRAGE: TR = 1620 ms, TI = 950 ms, TE = 3 ms, flip angle = 15º, 160 contiguous slices of 1.0 mm thickness, FOV = 192 × 256 mm^2, matrix = 192 × 256, 1NEX with a scan time of 6 min.

Behavioral data analysis

Performance of the subjects was characterized with respect to three dimensions: discrimination, response bias, and speed. Discrimination was measured with d′. Response bias was characterized by yes rate (total proportion of button presses without regard to accuracy). Speed was operationalized as median RT on hits (correct button presses to targets).

Imaging data analysis

Functional image pre-processing and individual-level analysis were carried out using VoxBo software (Center for Functional Neuroimaging, Philadelphia, PA, http://www.voxbo.org). The group-level analysis was performed with Statistical Parametric Mapping software (SPM99, Wellcome Department of Cognitive Neurology, London, UK, http://www.fil.ion.ucl.ac.uk/spm) . For each subject, functional images were realigned to correct the head motion using a 6-parameter rigid-body least squares realignment routine (Friston et al., 1995). Subjects who showed excessive head motion, defined as any translational movement larger than 2 voxels along the *x* or *y* axis or 1 voxel size along the *z* axis, were excluded from further analysis ($n = 5$). Realigned images were smoothed in space with a three-dimensional Gaussian kernel (4 × 4 × 3 voxels at FWHM). Perfusion-weighted image series were generated by pairwise subtraction of the label and control images followed by conversion to absolute CBF image series based on a single compartment CASL perfusion model (Wang et al., 2005). The resulting CBF data sets contained 46 images for each 6-min task block with an effective TR of 8 s. The CBF images were then normalized to a 3 × 3 × 3mm^3 Montreal Neurological Institute (MNI) template using bilinear interpolation.

For each cognitive task, the following statistical analyses were conducted. First, for each subject, voxel-wise individual GLMs were built comparing each task condition with the resting baseline by using appropriately weighted linear contrasts. The global signal covariate was included in the GLM to reduce spatially coherent noise in the data (Aguirre et al., 1998). The perfusion MRI data are known to be free from any substantial temporal autocorrelation (Aguirre et al., 2002; Wang et al., 2003a,b). Therefore, no filtering, autocorrelation modeling, or smoothing was done for the time series. The resulting parameter estimates were then fed into a random effects model to allow population-level inferences (Holmes and Friston, 1998). Areas of significant activation were identified at the cluster level (Forman et al., 1995) for the *P* value smaller than 0.005 ($t = 3.11$) and the cluster extent size larger than 50 voxels. These criteria yielded a level of $P < 0.005$ for each significant cluster after correction for multiple comparisons. The resultant activation clusters were used as functionally defined regions of interest (ROIs) for the subsequent ROI analysis.

A public domain software package MRIcro (http://www.psychology.nottingham.ac.uk/staff/cr1/mricro.html) was used to project group activation data to the Colin-brain atlas (Van Essen et al., 2001) in MNI space for display purposes. Activation peaks in MNI space were converted to Talaraich coordinates (Talairach and Trounoux, 1988) to allow better comparison with locations of activations from previous studies. This non-linear conversion was achieved using a MATLAB program provided with SPM extensions (http://www.mrc-cbu.cam.ac.uk/Imaging/Common/ mnispace.shtml). Anatomical labels for these activation peaks were determined using the Talairach Daemon (Lancaster et al., 2000). To calculate the mean CBF increase (and % CBF change equivalent) of activation relative to the resting baseline, the adjusted (for the global signal) CBF time series for each voxel from each subject was averaged across all the voxels in each ROI and then averaged across subjects.

Results

Behavioral results

Subjects performed the visual target detection task with a d′ (mean ± standard deviation) of 1.41 ± 1.11 and an RT of 979 ± 362 ms. The yes rate was 0.29 ± 0.12 (where target rate = 20%). The d′ and the RT of the 2-back task were 3.03 ± 1.06 and 717 ± 137 ms. The yes rate was 0.12 ± 0.02 (where target rate = 12%).

Imaging results

Fig. 1 shows the quantitative mean CBF images in a representative subject, with fourteen slices covering

the whole brain from the top of the brain to the cerebellum. Without using a separate labeling coil, we were able to obtain clear quantitative perfusion contrasts of the gray and white matter. The calculated mean CBF of the group (n = 12) was 51.69 ml/100 g/min ± 12.7 for the whole brain, which is comparable to previously reported mean CBF values for the whole brain using PET and ASL methods (e.g., Lassen, 1985; Yee et al., 2000).

Significant task-related CBF changes were observed in many hypothesized areas for each task. Tables 1 and 2 list the clusters showing significant CBF changes for each task. The coordinates of the local maxima and percent CBF changes associated with each region are also reported. Fig. 2 illustrates resampled axial images of the activated areas for the two tasks.

For the visual sustained attention task, four activated clusters were identified including the right middle frontal gyrus (BA 9), bilateral occipital gyri (BA 18), and the anterior cingulate/medial frontal gyrus (BA 32/8) (Fig. 2; Table 1). All of these areas showed increased CBF during performance of the visual attention task relative to the resting baseline. In addition to these activated areas, there were 'de-activated' regions more active in the resting baseline compared to the active task block. These areas included the left superior/middle temporal gyri, the bilateral posterior cingulate gyri, and the right superior/medial frontal gyrus. As shown in Table 1, the magnitude of % CBF changes ranged from 9 to 23% (6-12 ml/100 g/min) at the cluster level. Sizes of the ROIs and standard deviations of the CBF values are also reported.

For the letter 2-back task, the task versus resting contrast showed strong left-hemispheric lateralization with activation in the left inferior frontal/precentral gyri (BA 9/6), the left inferior parietal lobule (BA 40), the left middle occipital gyrus (BA 37), and the anterior cigulate/medial frontal gyri (BA 32/6) (Fig. 2; Table 2). Regions that were deactivated during the task block compared to the baseline included bilateral posterior cingulated/medial frontal gyri, bilateral superior/middle temporal gyri, bilateral posterior insular cortices, and the left superior frontal gyrus. As shown in the Table 2, the magnitude of % CBF changes ranged from 10 to 26% (7 – 11 m./100 g/min) at the cluster level.

Discussion

The purpose of the present study was to demonstrate the feasibility of CASL perfusion fMRI for the investigation of higher cognitive processes. Utilizing our amplitude-modulated CASL MRI imaging protocol with a single coil at 3 T field strength (Wang et al., 2005), we were able to characterize tonic CBF changes associated with an uninterrupted 6 min continuous performance of the two high-level cognitive tasks—i.e., visual sustained attention and verbal working memory. Appropriate image quality and whole brain coverage were obtained without using any additional hardware, such as a separate labeling coil (Talagala et al., 2004; Zaharchuk et al., 1999).

Activated areas of the two tasks largely coincided with the regions in similar tasks from prior neuroimaging studies. For the 2-back task, we found a left-hemisphere dominant activation pattern throughout the fronto-parietal 'working memory network' (Klingberg et al., 1997). Recently, Owen and colleagues provided a metaanalysis of neuroimaging studies that used variants of the n-back task (Owen et al., 2005). Among the studies reviewed in the article, we selected 11 studies that included a verbal 2-back condition. Then, we made a list of activated regions from those studies to compare them with the activated areas of the present study. It was found that every activated area found in our study (Table 2) was also reported as a significant activation focus in one or more previous studies of the verbal 2-back task (Awh et al., 1996; Braver et al., 1997; Cohen et al., 1994, 1997; Honey et al., 2000; Jonides et al., 1997; Kim et al., 2002; Nystrom et al., 2000; Ragland et al., 2002; Smith et al., 1996; Veltman et al., 2003).

The strong laterality effects observed in the current study support the domain dominance hypothesis of working memory stating that verbal memory involves predominantly left hemisphere while spatial memory mainly involves right hemisphere (Smith et al., 1996). However, it is possible that the observed laterality is a result of a lack of power to detect activations in the right hemisphere. To test this hypothesis, a new voxel-wise group analysis was performed using a more lenient threshold ($P < 0.01$, uncorrected for multiple comparison). The new statistical parametric map additionally revealed subthreshold activations (Z values near 3.0) in the right middle frontal/precentral (BA 6) and the right inferior parietal (BA 40) regions, supporting the notion that the laterality effects are quantitative rather than qualitative (Walter et al., 2003).

For the visual sustained attention task, a right-hemisphere dominant activation pattern was found in the middle frontal gyrus (BA 9), the occipital gyri (BA 18), and the anterior cingulate/ medial frontal gyrus (BA 32/8). Each of these areas was also reported as an activation focus in one or more of the prior studies of visual sustained attention (Coull et al., 1996, 1998; Lawrence et al., 2003; Pardo et al., 1991). However, there was a potentially interesting difference between our study and previous studies of visual sustained attention: the right parietal activation reported in most of the prior studies was not found in the present study. Employing a more lenient threshold ($P < 0.01$, uncorrected) did not reveal a subthreshold cluster of parietal activation. We speculate on two possible explanations. One is simply that the parietal activation seen in previous BOLD studies could be associated with target detection, rather than the continuous task set of sustained attentiveness, and thus might be more transient than the right frontal activation. In that case, transient neural activations in parietal cortex might have not been detected due to the rather long ISI (6 s) combined with the slow data acquisition rate (8 s effective TR). A second possibility is that the activation of parietal cortex in sustained attention tasks reflects the confounding with working memory processes. In fact, sustained attention and working memory are frequently difficult to disentangle. Sustained attention tasks used in most previous studies had strong working memory components, such as updating consecutive digits (Coull et al., 1996; Lawrence et al., 2003) or counting certain types of events (Pardo et al., 1991). If parietal activation in those studies reflected maintenance processes of working memory (e.g., Jonides et al., 1998; Mannan et al., 2005; Ravizza et al., 2005), lack of parietal activation in the present study may be due to the fact that our visual target detection task required minimal working memory load.

The areas of deactivation largely concur with previous studies (Binder et al., 1999; Mazoyer et al., 2001; Shulman et al., 1997). Deactivated areas included the superior/middle temporal gyrus (BA 21/22), the posterior cingulate (BA 24), and the superior frontal gyrus (BA 10). Different from the activated areas, deactivated foci showed a large overlap between two tasks, supporting the existence of a common 'default' network (Gusnard and Raichle, 2001). The only difference is the fact that the 2-back task showed larger and more bilateral areas of deactivation compared to the visual sustained attention task.

Percent CBF changes during the visual sustained attention task ranged from 9 to 23% (6–12 ml/100 g/min), based on the functionally defined ROIs in normalized space. Previous PET studies of visual sustained attention (Coull et al., 1996, 1998; Pardo et al., 1991) typically did not report mean CBF increases or % CBF changes for activated regions due to their global normalization procedure (e.g., artificially setting the global signal to 50 ml/100 g/min), precluding comparison with the current findings. For the 2-back task, we found % CBF changes ranging from 10 to 26% (7 –11 ml/100 g/min). Some PET studies reported 2–7% CBF changes for the 2-back condition compared to the 0back control (e.g., Jonides et al., 1997; Kim et al., 2003). However, % CBF changes are likely to be influenced by many factors such as the nature of the control condition, the sizes of smoothing kernels and ROIs and whether normalization was done or not. Thus, cautious efforts to exactly replicate prior studies in terms of data acquisition and imaging analysis parameters are needed in the future to make precise comparisons of % CBF change values between studies.

Several limitations of the present study should be recognized. First, the temporal resolution of the current CASL method was rather low compared to that of a BOLD fMRI experiment, which has typically a TR of 2 - 4 s. However, for some research questions, this limitation is outweighed by the CASL technique's ability to measure activation associated with prolonged mental activity and tonic task sets, as well as its ability to study longitudinal change in performance during learning or neurologic recovery, and its ability to distinguish the direct cardiovascular effects of psychoactive drugs from secondary effects related to changes in cognitive processing. In addition, novel labeling paradigms have been proposed recently to improve the temporal resolution of ASL methods, even allowing event-related fMRI designs (Wong et al., 2000; Yang et al., 2000).

Another potential limitation of the present study is related to the nature of the resting condition used as the baseline. We used a resting condition with closed eyes because this condition could yield a physiological baseline (Gusnard and Raichle, 2001), and it was used as a control condition for a majority of previous PET studies of sustained attention (Coull et al., 1996; Kinomura et al., 1996; Pardo et al., 1991). In fact, one might argue that the resting baseline is most suitable for a sustained attention task since most control tasks would also induce a sustained attention load. However, utilizing a more specific control condition such as 0-back, 1-back, or variants of visual fixation will eventually be more helpful in isolating specific cognitive processes. It still remains as an empirical question whether CASL perfusion fMRI can detect subtle condition differences to isolate more specific subcomponents of higher cognition.

Lastly, one can be concerned about the fixed order of the task blocks in the current study since time-dependent physiologic noise such as fatigue or adaptation effects might have affected the results. However, these effects, if any, did not prevent us from finding distinct activation patterns of the two tasks. Good agreement on activation sites with previous studies of each task also indicates that observed activation differences between the two tasks are not merely due to the time-related effects.

ASL perfusion fMRI is a completely non-invasive technique that shows the capability to quantify absolute CBF and stable noise characteristics over the entire spectrum. CBF measurements with ASL perfusion MRI have recently been shown to agree with results from ^{15}O-PET (Ye et al., 2000) and dynamic susceptibility contrast agent approach (Siewert et al., 1997; Wolf et al., 2003). ASL perfusion measurements both at rest and during task activation have also been demonstrated to be highly reproducible across intervals varying from a few minutes to a few days (Floyd et al., 2003; Wang et al., 2003a,b). In addition, as reviewed in Introduction, this method may provide (1) reduced motion and susceptibility artifacts in regions of high static inhomogeneity, (2) smaller intersubject variance, and (3) potentially greater spatial resolution. On the other hand, the current state of the method has several technical limitations including (1) fewer number of slices, (2) low temporal resolution, and (3) relatively low SNR. Because of its superior sensitivity, BOLD fMRI will be the method of choice when a maximum detection power is needed and when the subject of interest is the processing of specific events. However, due to the merits mentioned above and continuing technical improvements to come, ASL perfusion fMRI will be increasingly used for basic and clinical neuroimaging applications, particularly when longitudinal stability (e.g., studies of drug treatment or training effects) and slow changes in mental state (e.g., task set, learning, emotion, and sustained attention) are of interest. The present study has for the first time demonstrated that the CASL perfusion fMRI methodology can be successfully utilized for the study of higher cognition such as sustained attention and working memory. An extensive number of ASL studies of higher cognitive processes in healthy and clinical populations are expected to be seen in the near future.

Acknowledgments

The authors wish to thank Daniel Kimberg, Ph.D. and Geoffrey K. Aguirre, MD, Ph.D. for their helpful comments on data analysis and Monica Vaccaro, M.A. for her help in subject screening. The assistance of MRI technician Doris Cain is also gratefully acknowledged. This study is supported by grant R24HD39621 from the NCMRR, NICHD, NIH, and P30NS045839 from the NINDS, NIH. This project is also funded, in part, under a grant with the Pennsylvania Department of Health. The Department specifically disclaims responsibility for any analyses, interpretations, or conclusions.

References

Aguirre, G.K., Zarahn, E., D'Esposito, M., 1998. The inferential impact of global signal covariates in functional neuroimaging analyses. Neuro-Image 8 (3), 302 –306.

Aguirre, G.K., Detre, J.A., Zarahn, E., Alsop, D.C., 2002. Experimental design and the relative sensitivity of BOLD and perfusion fMRI. NeuroImage 15 (3), 488 –500.

Ances, B.M., McGarvey, M.L., Abrahams, J.M., Maldjian, J.A., Alsop, D.C., Zager, E.L., et al., 2004. Continuous arterial spin labeled perfusion magnetic resonance imaging in patients before and after carotid endarterectomy. J. Neuroimaging 14 (2), 133 –138.

Awh, E., Jonides, J., Smith, E.E., Schumacher, E.H., Koeppe, R.A., Katz, S., 1996. Dissociation of storage and rehearsal in verbal working memory: evidence from positron emission tomography. Psychol. Sci. 7 (1), 25 –31.

Binder, J.R., Frost, J.A., Hammeke, T.A., Bellgowan, P.S., Rao, S.M., Cox, R.W., 1999. Conceptual processing during the conscious resting state. A functional MRI study. J. Cogn. Neurosci. 11 (1), 80 –95.

Braver, T.S., Cohen, J.D., Nystrom, L.E., Jonides, J., Smith, E.E., Noll, D.C., 1997. A parametric study of prefrontal cortex involvement in human working memory. NeuroImage 5 (1), 49 –62.

Cabeza, R., Nyberg, L., 2000. Imaging cognition: II. An empirical review of 275 PET and fMRI studies. J. Cogn. Neurosci. 12 (1), 1–47.

Calamante, F., Thomas, D.L., Pell, G.S., Wiersma, J., Turner, R., 1999. Measuring cerebral blood flow using magnetic resonance imaging techniques. J. Cereb. Blood Flow Metab. 19 (7), 701 –735.

Callicott, J.H., Mattay, V.S., Verchinski, B.A., Marenco, S., Egan, M.F., Weinberger, D.R., 2003. Complexity of prefrontal cortical dysfunction in schizophrenia: more than up or down. Am. J. Psychiatry 160 (12), 2209–2215.

Cohen, J.D., Forman, S.D., Braver, T.S., Casey, B.J., Servan-Schreiber, D., Noll, D.C., 1994. Activation of the prefrontal cortex in a nonspatial working memory task with functional MRI. Hum. Brain Mapp. 1 (4), 293–304.

Cohen, J.D., Perlstein, W.M., Braver, T.S., Nystrom, L.E., Noll, D.C., Jonides, J., et al., 1997. Temporal dynamics of brain activation during a working memory task. Nature 386 (6625), 604 –608.

Colebatch, J.G., Deiber, M.P., Passingham, R.E., Friston, K.J., Frackowiak, R.S., 1991. Regional cerebral blood flow during voluntary arm and hand movements in human subjects. J. Neurophysiol. 65 (6), 1392 –1401.

Coull, J.T., Frith, C.D., Frackowiak, R.S., Grasby, P.M., 1996. A frontoparietal network for rapid visual information processing: a PET study of sustained attention and working memory. Neuropsychologia 34 (11), 1085–1095.

Coull, J.T., Frackowiak, R.S., Frith, C.D., 1998. Monitoring for target objects: activation of right frontal and parietal cortices with increasing time on task. Neuropsychologia 36 (12), 1325–1334.

D'Esposito, M., Aguirre, G.K., Zarahn, E., Ballard, D., Shin, R.K., Lease, J., 1998. Functional MRI studies of spatial and nonspatial working memory. Brain Res. Cogn. Brain Res. 7 (1), 1 –13.

Detre, J.A., Alsop, D.C., 1999. Perfusion magnetic resonance imaging with continuous arterial spin labeling: methods and clinical applications in the central nervous system. Eur. J. Radiol. 30 (2), 115 – 124.

Detre, J.A., Floyd, T.F., 2001. Functional MRI and its applications to the clinical neurosciences. Neuroscientist 7 (1), 64 –79.

Detre, J.A., Wang, J., 2002. Technical aspects and utility of fMRI using BOLD and ASL. Clin. Neurophysiol. 113 (5), 621 –634.

Detre, J.A., Leigh, J.S., Williams, D.S., Koretsky, A.P., 1992. Perfusion imaging. Magn. Reson. Med. 23 (1), 37 –45.

Duong, T.Q., Kim, D.S., Ugurbil, K., Kim, S.G., 2001. Localized cerebral blood flow response at submillimeter columnar resolution. Proc. Natl. Acad. Sci. U. S. A. 98 (19), 10904 –10909.

Floyd, T.F., Ratcliffe, S.J., Wang, J., Resch, B., Detre, J.A., 2003. Precision of the CASL-pefusion MRI technique: global and regional cerebral blood flow within vascular territories at one hour and one week. J. Magn. Reson. Imaging 18, 649 –655.

Forman, S.D., Cohen, J.D., Fitzgerald, M., Eddy, W.F., Mintun, M.A., Noll, D.C., 1995. Improved assessment of significant activation in functional magnetic resonance imaging (fMRI): use of a cluster-size threshold. Magn. Reson. Med. 33 (5), 636 –647.

Friston, K.J., Ashburner, J., Frith, C.D., Poline, J.-B., Heather, J.D., 1995. Spatial normalization and registration of images. Hum. Brain Mapp. 3, 165–189.

Friston, K.J., Josephs, O., Zarahn, E., Holmes, A.P., Rouquette, S., Poline, J., 2000. To smooth or not to smooth? Bias and efficiency in fMRI time-series analysis. NeuroImage 12 (2), 196 –208.

Garraux, G., Hallett, M., Talagala, S.L., 2005. CASL fMRI of subcorticocortical perfusion changes during memory-guided finger sequences. NeuroImage 25 (1), 122 –132.

Gusnard, D.A., Raichle, M.E., 2001. Searching for a baseline: functional imaging and the resting human brain. Nat. Rev., Neurosci. 2 (10), 685 –694.

Hennig, J., Speck, O., Koch, M.A., Weiller, C., 2003. Functional magnetic resonance imaging: a review of methodological aspects and clinical applications. J. Magn. Reson. Imaging 18 (1), 1 –15.

Holmes, A., Friston, K.J., 1998. Generalizability, random effects, and population inference. NeuroImage 7, S754.

Honey, G.D., Bullmore, E., 2004. Human pharmacological MRI. Trends Pharmacol. Sci. 25 (7), 366 –374.

Honey, G.D., Bullmore, E.T., Sharma, T., 2000. Prolonged reaction time to a verbal working memory task predicts increased power of posterior parietal cortical activation. NeuroImage 12 (5), 495 –503.

Johnson, N.A., Jahng, G.H., Weiner, M.W., Miller, B.L., Chui, H.C., Jagust, W.J., et al., 2005. Pattern of cerebral hypoperfusion in Alzheimer disease and mild cognitive impairment measured with arterial spin-labeling MR imaging: initial experience. Radiology 234 (3), 851 –859.

Jonides, J., Schumacher, E.H., Smith, E.E., Lauber, E.J., et al., 1997. Verbal working memory load affects regional brain activation as measured by PET. J. Cogn. Neurosci. 9 (4), 462 –475.

Jonides, J., Schumacher, E.H., Smith, E.E., Koeppe, R.A., Awh, E., Reuter-Lorenz, P.A., et al., 1998. The role of parietal cortex in verbal working memory. J. Neurosci. 18 (13), 5026 –5034.

Kemeny, S., Ye, F.Q., Birn, R., Braun, A.R., 2005. Comparison of continuous overt speech fMRI using BOLD and arterial spin labeling. Hum. Brain Mapp. 24 (3), 173 –183.

Kim, J.J., Kim, M.S., Lee, J.S., Lee, D.S., Lee, M.C., Kwon, J.S., 2002. Dissociation of working memory processing associated with native and second languages: PET investigation. NeuroImage 15 (4), 879 –891.

Kim, J.J., Kwon, J.S., Park, H.J., Youn, T., Kang do, H., Kim, M.S., et al., 2003. Functional disconnection between the prefrontal and parietal cortices during working memory processing in schizophrenia: a[15(O)]H2O PET study. Am. J. Psychiatry 160 (5), 919 –923.

Kinomura, S., Larsson, J., Gulyas, B., Roland, P.E., 1996. Activation by attention of the human reticular formation and thalamic intralaminar nuclei. Science 271 (5248), 512 –515.

Klingberg, T., O'Sullivan, B.T., Roland, P.E., 1997. Bilateral activation of fronto-parietal networks by incrementing demand in a working memory task. Cereb. Cortex 7 (5), 465 –471.

Kwon, H., Menon, V., Eliez, S., Warsofsky, I.S., White, C.D., Dyer-Friedman, J., et al., 2001. Functional neuroanatomy of visuospatial working memory in fragile X syndrome: relation to behavioral and molecular measures. Am. J. Psychiatry 158 (7), 1040 –1051.

Kwong, K.K., Belliveau, J.W., Chesler, D.A., Goldberg, I.E., Weisskoff, R.M., Poncelet, B.P., et al., 1992. Dynamic magnetic resonance imaging of human brain activity during primary sensory stimulation. Proc. Natl. Acad. Sci. U. S. A. 89 (12), 5675 –5679.

Lancaster, J.L., Woldorff, M.G., Parsons, L.M., Liotti, M., Freitas, C.S., Rainey, L., et al., 2000. Automated Talairach atlas labels for functional brain mapping. Hum. Brain Mapp. 10 (3), 120 –131.

Lassen, N.A., 1985. Normal average value of cerebral blood flow in younger adults is 50 ml/100 g/min. J. Cereb. Blood Flow Metab. 5 (3), 347–349.

Lawrence, N.S., Ross, T.J., Hoffmann, R., Garavan, H., Stein, E.A., 2003. Multiple neuronal networks mediate sustained attention. J. Cogn. Neurosci. 15 (7), 1028 –1038.

Luh, W.M., Wong, E.C., Bandettini, P.A., Ward, B.D., Hyde, J.S., 2000. Comparison of simultaneously measured perfusion and BOLD signal increases during brain activation with T(1)-based tissue identification. Magn. Reson. Med. 44 (1), 137 –143.

Mandeville, J.B., Marota, J.J., Ayata, C., Moskowitz, M.A., Weisskoff, R.M., Rosen, B.R., 1999. MRI measurement of the temporal evolution of relative CMRO (2) during rat forepaw stimulation. Magn. Reson. Med. 42 (5), 944 –951.

Mannan, S.K., Mort, D.J., Hodgson, T.L., Driver, J., Kennard, C., Husain, M., 2005. Revisiting previously searched locations in visual neglect: role of right parietal and frontal lesions in misjudging old locations as new. J. Cogn. Neurosci. 17 (2), 340 –354.

Matthews, P.M., Jezzard, P., 2004. Functional magnetic resonance imaging. J. Neurol., Neurosurg. Psychiatry 75 (1), 6 –12.

Mazoyer, B., Zago, L., Mellet, E., Bricogne, S., Etard, O., Houde, O., et al., 2001. Cortical networks for working memory and executive functions sustain the conscious resting state in man. Brain Res. Bull. 54 (3), 287 –298.

Mildner, T., Trampel, R., Moller, H.E., Schafer, A., Wiggins, C.J., Norris, D.G., 2003. Functional perfusion imaging using continuous arterial spin labeling with separate labeling and imaging coils at 3 T. Magn. Reson. Med. 49 (5), 791 –795.

Nystrom, L.E., Braver, T.S., Sabb, F.W., Delgado, M.R., Noll, D.C., Cohen, J.D., 2000. Working memory for letters, shapes, and locations: fMRI evidence against stimulus-based regional organization in human prefrontal cortex. NeuroImage 11 (5 Pt. 1), 424 –446.

Ogawa, S., Menon, R.S., Tank, D.W., Kim, S.G., Merkle, H., Ellermann, J.M., et al., 1993. Functional brain mapping by blood oxygenation level-dependent contrast magnetic resonance imaging. A comparison of signal characteristics with a biophysical model. Biophys. J. 64 (3), 803 –812.

Oguz, K.K., Golay, X., Pizzini, F.B., Freer, C.A., Winrow, N., Ichord, R., et al., 2003. Sickle cell disease: continuous arterial spin-labeling perfusion MR imaging in children. Radiology 227 (2), 567–574.

Oldfield, R.C., 1971. The assessment and analysis of handedness: the Edinburgh inventory. Neuropsychologia 9 (1), 97 –113.

Owen, A.M., McMillan, K.M., Laird, A.R., Bullmore, E., 2005. N-back working memory paradigm: a meta-analysis of normative functional neuroimaging studies. Hum. Brain Mapp. 25 (1), 46 –59.

Pardo, J.V., Fox, P.T., Raichle, M.E., 1991. Localization of a human system for sustained attention by positron emission tomography. Nature 349 (6304), 61–64.

Paulesu, E., Frith, C.D., Frackowiak, R.S., 1993. The neural correlates of the verbal component of working memory. Nature 362 (6418), 342 –345.

Poldrack, R.A., 2000. Imaging brain plasticity: conceptual and methodological issues—A theoretical review. NeuroImage 12 (1), 1 –13.

Ragland, J.D., Turetsky, B.I., Gur, R.C., Gunning-Dixon, F., Turner, T., Schroeder, L., et al., 2002. Working memory for complex figures: an fMRI comparison of letter and fractal n-back tasks. Neuropsychology 16 (3), 370 –379.

Ramsey, N.F., Kirkby, B.S., Van Gelderen, P., Berman, K.F., Duyn, J.H., Frank, J.A., et al., 1996. Functional mapping of human sensorimotor cortex with 3D BOLD fMRI correlates highly with H2(15)O PET rCBF. J. Cereb. Blood Flow Metab. 16 (5), 755 –764.

Rashid, W., Parkes, L.M., Ingle, G.T., Chard, D.T., Toosy, A.T., Altmann, D.R., et al., 2004. Abnormalities of cerebral perfusion in multiple sclerosis. J. Neurol., Neurosurg. Psychiatry 75 (9), 1288 –1293.

Ravizza, S.M., Behrmann, M., Fiez, J.A., 2005. Right parietal contributions to verbal working memory: Spatial or executive? Neuropsychologia 43 (14), 2057 –2067.

Scheibel, R.S., Pearson, D.A., Faria, L.P., Kotrla, K.J., Aylward, E., Bachevalier, J., et al., 2003. An fMRI study of executive functioning after severe diffuse TBI. Brain Inj. 17 (11), 919 –930.

Shulman, G.L., Corbetta, M., Buckner, R.L., Fiez, J.A., Miezin, F.M., Raichle, M.E., et al., 1997. Common blood flow changes across visual tasks: I. Increases in subcortical structures and cerebellum but not in nonvisual cortex. J. Cogn. Neurosci. 9 (5), 624 –647.

Siewert, B., Schlaug, G., Edelman, R.R., Warach, S., 1997. Comparison of EPISTAR and T2*-weighted gadolinium-enhanced perfusion imaging in patients with acute cerebral ischemia. Neurology 48, 673–679.

Smith, E.E., Jonides, J., 1998. Neuroimaging analyses of human working memory. Proc. Natl. Acad. Sci. U. S. A. 95 (20), 12061–12068. Smith, E.E., Jonides, J., 1999. Storage and executive processes in the frontal lobes. Science 283 (5408), 1657 –1661.

Smith, E.E., Jonides, J., Koeppe, R.A., 1996. Dissociating verbal and spatial working memory using PET. Cereb. Cortex 6 (1), 11 –20.

Sweet, L.H., Rao, S.M., Primeau, M., Mayer, A.R., Cohen, R.A., 2004. Functional magnetic resonance imaging of working memory among multiple sclerosis patients. J. Neuroimaging 14 (2), 150 –157.

Talagala, S.L., Noll, D.C., 1998. Functional MRI using steady-state arterial water labeling. Magn. Reson. Med. 39 (2), 179 –183.

Talagala, S.L., Ye, F.Q., Ledden, P.J., Chesnick, S., 2004. Whole-brain 3D perfusion MRI at 3.0 T using CASL with a separate labeling coil. Magn. Reson. Med. 52 (1), 131 –140.

Talairach, J., Trounoux, P., 1988. Co-Planar Stereotaxic Atlas of the Human Brain. Thieme Medical Publishers, New York.

Tjandra, T., Brooks, J.C., Figueiredo, P., Wise, R., Matthews, P.M., Tracey, I., 2005. Quantitative assessment of the reproducibility of functional activation measured with BOLD and MR perfusion imaging: implications for clinical trial design. NeuroImage 27 (2), 393 –401.

Valera, E.M., Faraone, S.V., Biederman, J., Poldrack, R.A., Seidman, L.J., 2005. Functional neuroanatomy of working memory in adults with attention-deficit/hyperactivity disorder. Biol. Psychiatry 57 (5), 439–447.

Van Essen, D.C., Lewis, J.W., Drury, H.A., Hadjikhani, N., Tootell, R.B., Bakircioglu, M., et al., 2001. Mapping visual cortex in monkeys and humans using surface-based atlases. Vision Res. 41 (10–11), 1359 –1378.

Veltman, D.J., Rombouts, S.A., Dolan, R.J., 2003. Maintenance versus manipulation in verbal working memory revisited: an fMRI study. NeuroImage 18 (2), 247 –256.

Walter, H., Bretschneider, V., Gron, G., Zurowski, B., Wunderlich, A.P., Tomczak, R., et al., 2003. Evidence for quantitative domain dominance for verbal and spatial working memory in frontal and parietal cortex. Cortex 39 (4 –5), 897 –911.

Wang, J., Alsop, D.C., Li, L., Listerud, J., Gonzalez-At, J.B., Schnall, M.D., et al., 2002. Comparison of quantitative perfusion imaging using arterial spinlabelingat1.5 and 4.0 Tesla.Magn.Reson.Med. 48 (2), 242 –254.

Wang, J., Aguirre, G.K., Kimberg, D.Y., Detre, J.A., 2003a. Empirical analyses of null-hypothesis perfusion FMRI data at 1.5 and 4 T. NeuroImage 19 (4), 1449–1462.

Wang, J., Aguirre, G.K., Kimberg, D.Y., Roc, A.C., Li, L., Detre, J.A., 2003b. Arterial spin labeling perfusion fMRI with very low task frequency. Magn. Reson. Med. 49 (5), 796 –802.

Wang, J., Li, L., Roc, A.C., Alsop, D.C., Tang, K., Butler, N.S., et al., 2004. Reduced susceptibility effects in perfusion fMRI with single-shot spin-echo EPI acquisitions at 1.5 Tesla. Magn. Reson. Imaging 22 (1), 1 –7.

Wang, J., Zhang, Y., Wolf, R.L., Roc, A.C., Alsop, D.C., Detre, J.A., 2005. Amplitude-modulated continuous arterial spin-labeling 3.0-T perfusion MR imaging with a single coil: feasibility study. Radiology 235 (1), 218– 228.

Whyte, J., Hart, T., Vaccaro, M., Grieb-Neff, P., Risser, A., Polansky, M., et al., 2004. Effects of methylphenidate on attention deficits after traumatic brain injury: a multidimensional, randomized, controlled trial. Am. J. Phys. Med. Rehabil. 83 (6), 401 –420.

Whyte, J., Polansky, M., Fleming, M., Coslett, H.B., Cavallucci, C., 1995. Sustained arousal and attention after traumatic brain injury. Neuropsychologia 33 (7), 797 –813.

Wilke, M., Holland, S.K., Myseros, J.S., Schmithorst, V.J., Ball Jr., W.S., 2003. Functional magnetic resonance imaging in pediatrics. Neuropediatrics 34 (5), 225 –233.

Williams, D.S., Detre, J.A., Leigh, J.S., Koretsky, A.P., 1992. Magnetic resonance imaging of perfusion using spin inversion of arterial water. Proc. Natl. Acad. Sci. U. S. A. 89 (1), 212 –216.

Wolf, R.L., Alsop, D.C., McGarvey, M.L., Maldjian, J.A., Wang, J., Detre, J.A., 2003. Susceptibility contrast and arterial spin labeled perfusion MRI in cerebrovascular disease. J. Neuroimaging 13 (1), 17–27.

Wong, E.C., Luh, W.M., Liu, T.T., 2000. Turbo ASL: arterial spin labeling with higher SNR and temporal resolution. Magn. Reson. Med. 44 (4), 511 –515.

Yang, Y., Engelien, W., Pan, H., Xu, S., Silbersweig, D.A., Stern, E., 2000. A CBF-based event-related brain activation paradigm: characterization of impulse-response function and comparison to BOLD. NeuroImage 12 (3), 287 –297.

Ye, F.Q., Berman, K.F., Ellmore, T., Esposito, G., van Horn, J.D., Yang, Y., et al., 2000. H(2)(15)O PET validation of steady-state arterial spin tagging cerebral blood flow measurements in humans. Magn. Reson. Med. 44 (3), 450 –456.

Ye, F.Q., Smith, A.M., Mattay, V.S., Ruttimann, U.E., Frank, J.A., Weinberger, D.R., et al., 1998. Quantitation of regional cerebral blood flow increases in prefrontal cortex during a working memory task: a steady-state arterial spin-tagging study. NeuroImage 8 (1), 44–49.

Yee, S.H., Liu, H.L., Hou, J., Pu, Y., Fox, P.T., Gao, J.H., 2000. Detection of the brain response during a cognitive task using perfusion-based event-related functional MRI. NeuroReport 11 (11), 2533 –2536.

Zaharchuk, G., Ledden, P.J., Kwong, K.K., Reese, T.G., Rosen, B.R., Wald, L.L., 1999. Multislice perfusion and perfusion territory imaging in humans with separate label and image coils. Magn. Reson. Med. 41 (6), 1093–1098.

Zarahn, E., Aguirre, G.K., D'Esposito, M., 1997. Empirical analyses of BOLD fMRI statistics. I. Spatially unsmoothed data collected under null-hypothesis conditions. NeuroImage 5 (3), 179 –197.

Figures and Tables

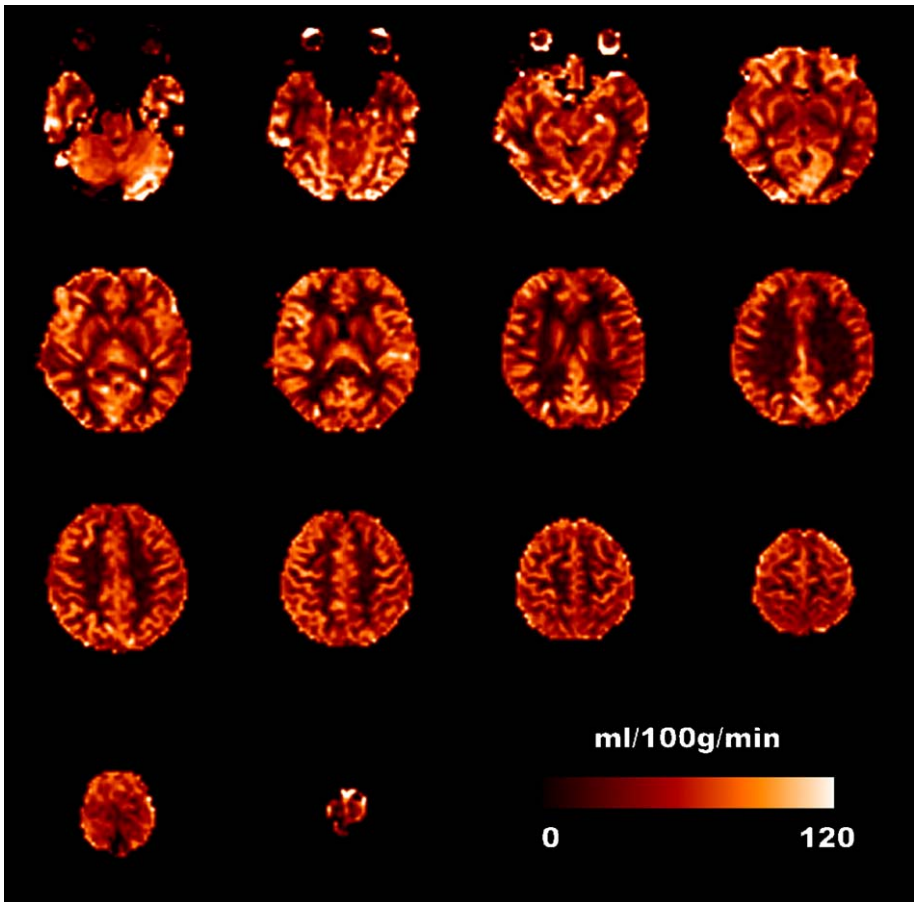

Fig. 1. Mean CBF images in a representative subject during the entire experiment. Total acquisition time was 18 min.

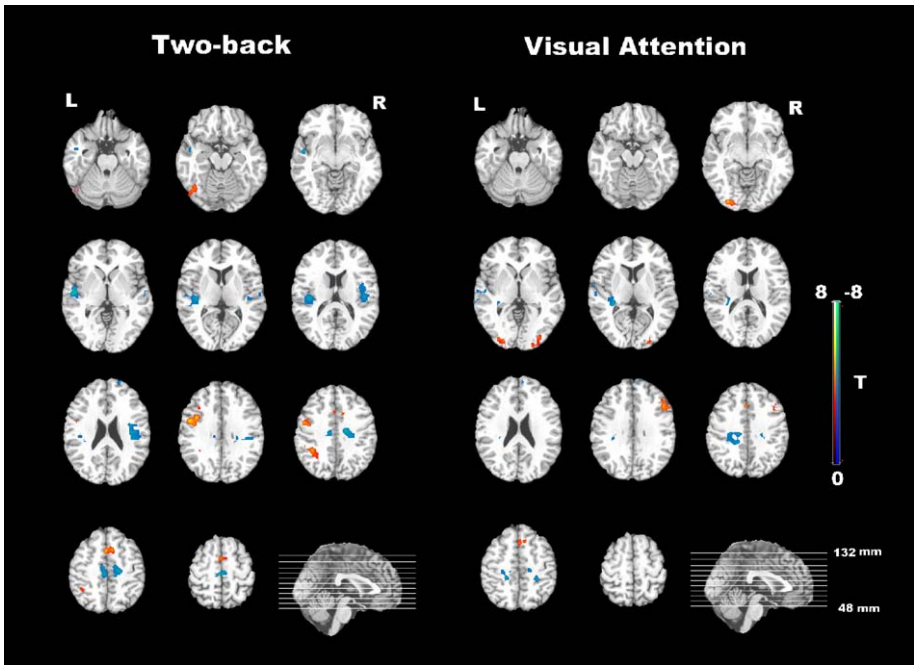

Fig. 2. Areas of significant CBF changes during the visual sustained attention and the 2-back task projected onto the Colin-brain atlas in MNI space. Activations are coded with hot colors (yellow and red) and deactivations cold colors (green and blue).

Table 1

Clusters of significant CBF changes during the visual sustained attention task compared to the resting baseline[a]

Type	Size (voxels)	Anatomical label	BA	Talairach coordinates			Z score	Δ CBF ± SD (ml/100 g/min)	% CBF change ± SD
				x	y	z			
Activation	113	R. middle frontal gyrus	9	45	22	29	3.64	7.6 ± 4.6	13.2 ± 7.2
	111	R. middle occipital gyrus	18	30	-84	2	3.28	12.1 ± 8.8	23.4 ± 18.6
		R. cuneus	18	18	-99	8	3.19		
	97	L. middle occipital gyrus	18	-33	-85	-1	3.81	10.8 ± 8.7	22.0 ± 20.1
	70	R. medial frontal gyrus	8	9	29	48	4.02	5.9 ± 5.3	9.2 ± 9.0
		L. cingulate gyrus	32	-6	22	38	3.79		
Deactivation	394	L. cingulate gyrus	24	-18	-18	40	4.01	-4.9 ± 2.3	-12.4 ± 7.9
		L. superior temporal gyrus	41	-33	-31	13	3.93		
		N/A	N/A	-33	-25	34	3.34		
	125	L. superior temporal gyrus	22	-65	-5	9	3.57	-7.1 ± 4.6	12.2 ± 7.7
		L. superior temporal gyrus	21	-53	-15	-2	3.21		
		L. middle temporal gyrus	21	-68	-26	-1	3.20		
	106	R. cingulate gyrus	24	15	-18	42	3.60	-6.0 ± 6.3	-13.4 ± 17.2
		R. postcentral gyrus	3	27	-33	49	3.49		
	53	R. superior frontal gyrus	10	12	62	25	3.27	-8.8 ± 6.4	-17.6 ± 16.6
		R. medial frontal gyrus	10	6	59	8	3.08		

[a] Cluster sizes are in voxels. Coordinates of local maxima at least 16 mm apart are reported per each cluster (maximum 3 maxima). The anatomical labels of the nearest gray matter within a 7 × 7 × 7 mm range were also reported. DCBF and % CBF values were calculated for each cluster. R. = Right. L. = Left. BA = Brodmann area. SD = standard deviation.

Table 2

Clusters of significant CBF changes during the 2-back task compared to the resting baseline[a]

Type	Size (voxels)	Anatomical label	BA	Talairach coordinates			Z score	Δ CBF ± SD (ml/100 g/min)	% CBF change ± SD
				x	y	z			
Activation	194	L. inferior parietal lobule	40	-50	-33	40	3.70	8.3 ± 6.1	15.7 (± 13.0)
		L. inferior parietal lobule	40	-33	-50	41	3.00		
	186	L. inferior frontal gyrus	9	-50	4	30	3.84	7.7 ± 5.0	14.1 (± 11.6)
		L. precentral gyrus	6	-39	22	27	2.84		
	141	L. medial frontal gyrus	6	-6	17	43	3.86	7.3 ± 4.2	11.5 (± 6.6)
		R. cingulated gyrus	32	9	14	38	3.60		
		L. medial frontal gyrus	6	-3	3	55	3.28		
	120	L. middle occipital gyrus	37	-48	-64	-7	3.27	11.1 ± 13.8[b]	26.0 (± 39.3)[b]
Deactivation	432	L. medial frontal gyurs	6	-6	-20	56	4.07	-5.6 ± 2.6	-12.1 (± 6.3)
		R. cingulated gyrus	24	12	-13	39	3.94		
		R. paracentral lobule	6	9	-24	51	3.74		
	399	R. insular	13	36	-5	20	3.65	-5.6 ± 2.7	-11.5 (± 6.1)
		R. insular	13	39	-22	29	3.54		
		R. superior temporal gyrus	22	62	3	-5	3.25		
	392	L. superior temporal gyrus	22	-53	-12	1	3.91	-6.9 ± 3.4	-10.2 (± 3.9)
		L. insular	13	-45	-20	15	3.63		
		L. middle temporal gyrus	21	-50	-1	-18	3.37		
	61	R. superior frontal gyrus	10	15	62	22	3.45	-6.5 ± 4.2	-13.5 (± 10.3)

[a] The details of this table are the same as those for Table 1.

[b] Based on $n = 11$. One subject's resting CBF value for this region showed extreme value due to artifacts and was excluded.